Original Article

The skin regeneration potential of a pro-angiogenic secretome from human skin-derived multipotent stromal cells

Journal of Tissue Engineering
Volume 10: 1–10

DOI: 10.1177/2041731419833391
journals.sagepub.com/home/tej
SAGE

Anny Waloski Robert[1], Felipe Azevedo Gomes[2], Michele Patricia Rode[2], Maiara Marques da Silva[2], Maria Beatriz da Rocha Veleirinho[2], Marcelo Maraschin[2], Leila Hayashi[2], Giordano Wosgrau Calloni[2] and Marco Augusto Stimamiglio[1]

Abstract

Multipotent stromal cells stimulate skin regeneration after acute or chronic injuries. However, many stem cell therapy protocols are limited by the elevated number of cells required and poor cell survival after transplantation. Considering that the beneficial effects of multipotent stromal cells on wound healing are typically mediated by paracrine mechanisms, we examined whether the conditioned medium from skin-derived multipotent stromal cells would be beneficial for restoring the skin structure of mice after wounding. A proteomic characterization of skin-derived multipotent stromal cell-conditioned medium was performed, and the angiogenic function of this secretome was investigated *in vitro* using an endothelial cell tube formation assay. We then applied the skin-derived multipotent stromal cell-conditioned medium directly to full-thickness excisional wounds or embedded it into carrageenan or poly(vinyl alcohol) hydrogels to monitor tissue regeneration in mice. Biological processes related to wound healing and angiogenesis were highlighted by the analysis of the skin-derived multipotent stromal cell secretome, and a pro-angiogenic capacity for promoting tubule-like structures was first confirmed *in vitro*. Skin wounds treated with skin-derived multipotent stromal cell-conditioned medium also displayed increased angiogenesis, independently of the association of the conditioned medium with hydrogels. However, improvements in wound closure and epidermis or decreased inflammatory cell presence were not observed. Hence, the use of the secretome obtained from human skin-derived multipotent stromal cells may be a potential strategy to aid the natural skin repair of full-thickness lesions mainly based on its pro-angiogenic properties.

Keywords

Secretome, skin-derived multipotent stromal cell, angiogenesis, wound healing

Date received: 10 September 2018; accepted: 26 January 2019

Introduction

The skin is the largest organ in human body, and it performs important functions such as protection, hydration maintenance, and thermoregulation. Superficial wounds heal by a natural repairing process; however, repair of acute or severe skin lesion in the dermal and epidermal layers is challenging.[1] Currently, the combinatorial use of three-dimensional biodegradable scaffolds, cells, and their derivatives has become attractive approaches for treating skin injuries.[2,3]

[1]Instituto Carlos Chagas, FIOCRUZ/PR, Curitiba, Brazil
[2]Federal University of Santa Catarina, Florianópolis, Brazil

Corresponding authors:
Giordano Wosgrau Calloni, Laboratory of Neural Crest Cells Plasticity and Differentiation, Federal University of Santa Catarina, Florianópolis, Santa Catarina, 88040-900, Brazil.
Email: giordano.calloni@ufsc.br

Marco Augusto Stimamiglio, Instituto Carlos Chagas, FIOCRUZ/PR, Rua Professor Algacyr Munhoz Mader, 3775, 81350-010, Curitiba, Paraná, Brazil.
Email: marco.stimamiglio@fiocruz.br

Thus, stem cell therapy, using multipotent stromal cells (MSCs), has been shown to modulate wound repair, inducing skin regeneration after acute or chronic injuries.[4,5] Among the sources of MSCs, skin-derived MSCs (SD-MSCs) are an option, since they are accessible by minimally invasive procedures, such as face-lifting surgery, also enabling autologous transplantation. Notably, the beneficial effects of MSCs on wound healing are typically mediated by paracrine mechanisms.[6,7] Thus, secreted factors obtained from cultured MSCs have been used as substitutes for numerous cell-based therapies.[3]

Previous studies have demonstrated that the conditioned medium (CM) from MSCs enhances the regeneration of skin lesions, as well as stimulates the migration of dermal cells, such as fibroblasts and keratinocytes, and promotes angiogenesis, both *in vitro* and *in vivo*.[8–11] Considering that the different tissue origins or culture conditions of MSCs may alter the profile of the secreted proteins (cell secretome), the CM derived from SD-MSCs (SD-MSC-CM) could be a singular source for skin regeneration. We therefore decided to examine whether SD-MSC-CM could be beneficial to the restoration of mouse skin structure and function after wounding. However, in an attempt to maintain the bioactive molecules of the CM at the wound site, the use of biocompatible hydrogels as carriers is desirable.[12,13]

Both natural hydrogels (e.g. alginate, chitosan, gelatin) and/or synthetic hydrogels (e.g. polyesters, polyacrylamide) are broadly used in tissue regeneration due to their ability to locally deliver entrapped bioactive molecules.[14] Carrageenans (CGs) are sulfated hydrophilic polysaccharides obtained from different red algae species and are extensively employed by the food industry[15] and in regenerative medicine as scaffolds and controlled-release systems for pharmaceutical drug delivery,[16] growth factors,[17] and cells.[18,19] Considering its potential, we previously used CG hydrogels in association with SD-MSC to treat skin lesions on a murine model of wound healing.[20] The combination of CG and SD-MSC were able to reduce inflammation, accelerate recovery, and increase the deposition of extracellular matrix at wounded area.[20] Similarly, polyvinyl alcohol (PVA) hydrogel is one of the most commonly used synthetic polymers for wound dressings and drug delivery.[21,22] PVA is a water soluble, non-toxic, biodegradable, and biocompatible polymer, which can form hydrogels via chemical or physical crosslinking, and it is also widely used in blends with other polymers and composites.[23,24] PVA is also a highly biocompatible excipient that enables CM absorption while maintaining structural integrity.[25]

Thus, the purpose of the present study was to evaluate the potential use of human SD-MSC-CM associated with a natural (CG) or a synthetic (PVA) polymer-based hydrogel to heal cutaneous wounds in mice. We first performed a proteomic characterization of the SD-MSC-CM and examined its potential to stimulate angiogenesis *in vitro*. Then, SD-MSC-CM was directly applied to the full thickness of excisional wounds or embedded into CG or PVA hydrogels to monitor tissue regeneration.

Materials and methods

Isolation and culture of human SD-MSCs

Human skin fragments from a face-lift were used to isolate SD-MSCs as previously reported.[26] These protocols were approved by the Human Ethics Committee of the Federal University of Santa Catarina (protocol 46674215.7.0000.0121). Briefly, human skin samples from three donors were maintained in Dulbecco's Modified Eagle's Medium (DMEM), digested with 12.5 U/mL dispase (BD Bioscience, San Diego, CA, USA), filtered through a 70-μm filter mesh and centrifuged at 300 *g* for 7 min. The cell pellet was suspended in DMEM supplemented with 10% fetal bovine serum (FBS) and cultivated at 37°C in a 5% CO_2 incubator until the preparation of the CM. The SD-MSCs used in the present study were previously characterized as MSCs.[20,26]

Preparation of the CM from SD-MSC cultures

SD-MSC cultures were maintained in DMEM supplemented with 10% FBS, 1% penicillin/streptomycin, and 1% L-glutamine until they reached 90% confluency. To collect the CM, the SD-MSC cultures were washed with phosphate buffered saline (PBS) and cultured for 10 days in DMEM without FBS. SD-MSC were tested to check viability and phenotypic changes before and after cultures, remaining viable and phenotypically unchanged during the assays (Supplementary Figure S1). After the media was collected, the samples were filtered through a 0.22-μm filter mesh and concentrated using centrifugal filter units with a 10-kDa cutoff (Merck Millipore, Darmstadt, Germany). The concentrated CM samples were stored at −80°C until further use. This procedure was performed with three distinct biological samples. The protein concentrations of all samples were measured by the bicinchoninic acid (BCA) Protein Assay Kit (Thermo Fisher Scientific, Waltham MA, USA). For functional assays, the SD-MSC-CM samples were pooled, and each treatment was performed with a total of 50 μg of protein.

Mass spectrometry and proteomic data analysis of the CM

Twenty micrograms of protein from each CM sample (three biological replicates and a technical replicate) were separated by 10% Sodium Dodecyl Sulfate–Polyacrylamide Gel Electrophoresis (SDS-PAGE). The gel lanes were excised and sliced, and the proteins were subjected to

in-gel tryptic digestion as previously described.[27] Five micrograms of extracted peptides were analyzed in triplicate by liquid chromatography–tandem mass spectrometry (LC-MS/MS) by using the Thermo Scientific Easy-nLC 1000 system coupled to an LTQ Orbitrap XL ETD system (Mass Spectrometry Facility RPT02H/Carlos Chagas Institute—Fiocruz-Parana, Brazil).

Data analysis were initiated by removing proteins identified "by site", potential contaminants, and reverse identifications. Then, for data interpretation, we considered only proteins with a minimum of two unique peptides that were identified in at least three samples. The Gene Ontology (GO) analysis was performed with g:Profiler bioinformatics toolkit (http://biit.cs.ut.ee/gprofiler/).[28] The most relevant terms ($p < 0.001$) identified by g:Profiler were summarized by REVIGO (http://revigo.irb.hr/).[29]

Hydrogel preparations and SD-MSC-CM incorporation

CG hydrogel was prepared and used as already standardized.[20] Shortly, the kappa-type CG (extracted from *Kappaphycus alvarezii* seaweed cultivated on the island of Florianópolis, Brazil) was used at 2% (w/v) in ultra-pure water after heating at 60°C for 30 min under stirring. The CG hydrogels were sterilized by steam power for 30 min at 120°C, filtered through a 0.8-µm filter mesh, polymerized in Lab-Tek® plates (8-well chamber slides; Thermo Fisher Scientific, Waltham MA, USA) and chopped with a 6-mm biopsy punch after polymerization (proportional to the excisional wound area in the animal model). The CM embedding (≈100 µL sample equivalent to 50 µg of protein) into the CG hydrogels was performed in a laminar flow chamber at 40°C to avoid the denaturation of CM proteins.

PVA hydrogel was prepared from suspensions of 20% (w/v; PVA M_w = 85,000–124,000; Merck KGaA, Darmstadt, Germany) in ultra-pure water incubated in a water bath at 85°C to 90°C under constant stirring. The obtained solution was placed in a glass Petri dish, autoclaved, and incubated at −20°C for 2 h to achieve polymerization in one cycle of freeze thawing as previously described.[24] The PVA hydrogel was cut with a 6-mm sterile biopsy punch in a laminar flow chamber, and each cylinder of PVA hydrogel was incubated overnight with the CM solution (≈100 µL sample equivalent to 50 µg of protein), which was fully incorporated into the hydrogel.

Human umbilical vein endothelial cell culture and in vitro tube formation assay

Human umbilical vein endothelial cells (HUVECs) were cultured according to the manufacturer's instructions (Lonza®, Basel, Switzerland; catalog number C2519A). Endothelial Cell Growth Basal Medium-2 (EBM-2) complete medium, supplemented with 5% FBS, human fibroblast growth factor b (hFGF-b), human epidermal growth factor (hEGF), human vascular endothelial cell growth factor (hVEGF), long R insulin-like growth factor-1 (R3-IGF-1), ascorbic acid, and hydrocortisone, was applied on expansion cultures. The cell cultures were maintained in a humidified atmosphere at 37ºC with 5% CO_2.

Tube formation assay using HUVECs was employed to verify the potential of CM to generate vessel-like structures *in vitro*. Briefly, 7×10^4 HUVECs/cm^2 were cultured on Matrigel® (Corning, Inc., Corning, New York, USA), and for treatments with CM, the equivalent to 50 µg of protein was applied to 500 µL of EBM-2 medium without supplementation. Positive controls received EBM-2 fully supplemented medium and negative controls received EBM-2 without any supplementation. After 12 and 24 h of culture, five randomly selected regions of the culture wells were photographed to manually count meshes and nodes.

In vivo cutaneous wound healing

The animal procedures were approved by the Ethics Committee on Animal Research of Federal University of Santa Catarina, Brazil (protocol number PP00810). The mouse model of cutaneous wound healing was adapted from the previously described protocol.[20] Briefly, C57BL/6 mice (4–5 months of age from both genders with body weights of 20–30 g) were anesthetized with ketamine (100 mg/kg) and xylazine (10 mg/kg) and had their dorsal region shaved. Subsequently, a full-thickness excisional wound diameter of 6 mm was produced with a sterile biopsy punch in the animal dorsum.[30]

The mice were subdivided into six experimental groups: control (CT; n = 12), which did not receive any treatment; CG hydrogel (CG; n = 9); CG hydrogel-embedded with SD-MSC-CM (CG + CM; n = 10); PVA hydrogel (PVA; n = 10); PVA hydrogel-embedded with SD-MSC-CM (PVA + CM; n = 11); and SD-MSC-CM only (CM; n = 8). The Tegaderm® (3M, St. Paul, MN, USA) transparent film was used to dress the wounds with a silicone ring sutured around the wound boundary. At 3 and 14 days post-treatment, the wounds were photographed, and their diameters were measured with ImageJ software.

Histopathological analysis

On days 3 and 14 post-treatment, the animals in each group were euthanized, and wound tissue samples were collected and fixed with 4% paraformaldehyde. The samples were then dehydrated in increasing concentrations of ethanol (70%–100%), cleared in xylol, embedded in paraffin, and sectioned (4 µm) for hematoxylin–eosin (H&E) staining. Inflammatory cell infiltration was assessed by estimating the leukocyte density at the site of the lesion at 3 days post-treatment. The inflammatory infiltration was classified

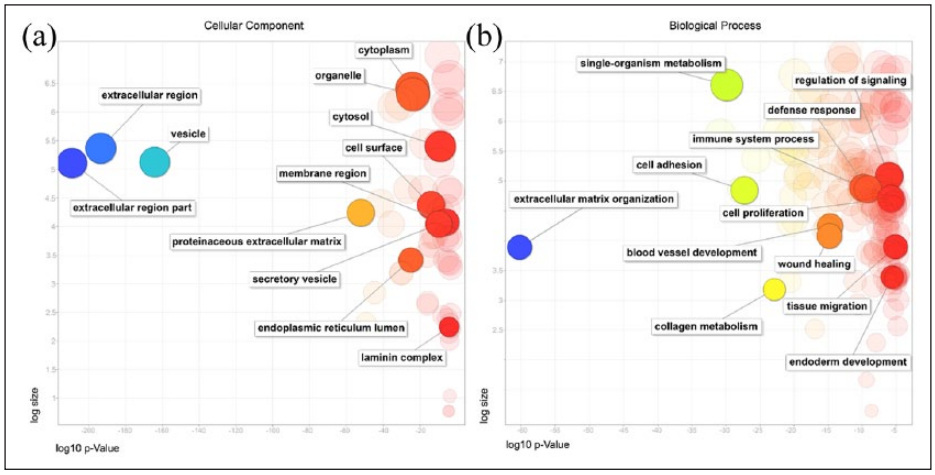

Figure 1. Gene ontology (GO) analysis of (a) cellular components and (b) biological processes based on the proteins identified in the SD-MSC secretome. A REVIGO scatterplot shows representative clusters of the GO analysis performed with g:Profiler. The log10 p-value of each GO term after REVIGO analysis is plotted on the x-axis, while the frequency of GO term in the GO Annotation Database is displayed on the y-axis (log size). Bubble colors indicate log10 p-value (from smaller p-values on blue color to highest p-values on red color).

into (1) low, (2) moderate, and (3) high levels of leukocyte density (represented in Supplementary Figure S2). Granulation tissue thickness, epidermal thickness, and uniformity were measured in H&E-stained sections from samples collected 14 days post-treatment. These measurements were performed using Zen software (Carl Zeiss Microscopy, Oberkochen, Germany) and analyzing five different sites of the wound. The epidermal uniformity parameter was obtained by considering the standard deviations of the thickness measurements. We also measured the density of blood vessels at the granulation tissue using ImageJ software. The analysis of blood vessels density was performed by counting the number of capillaries (containing a lumen with red blood cells) in each slide and calculating the mean number per animal. All analyzed images were obtained at 200× magnification.

Statistical analysis

Statistical analyses were performed using GraphPad Prism 7 software. Significant differences among treatments were evaluated using one-way analysis of variance (ANOVA), followed by Tukey's post hoc test. The data are expressed as the means ± standard deviation. Differences with $p < 0.05$ were considered statistically significant.

Results

The secretome profile of SD-MSCs exhibits proteins related to wound healing and blood vessel development

Human SD-MSCs were isolated and characterized by immunophenotyping and multilineage differentiation potential as previously described.[20,26] The cells were maintained in culture until the sixth passage, and then, the SD-MSC-CM was collected. SD-MSC cultures remained viable and phenotypically unchanged before and after CM collections (Supplementary Figure S1). Mass spectrometry analysis of SD-MSC-CM identified more than 300 proteins with a minimum of two unique peptides in each of the four samples (SD-MSC-CM 1–4). The complete list of identified proteins is available in Supplementary Table 1. Comparisons between the results showed that most of the proteins appeared in at least three of the four samples (a total of 399 proteins), indicating a robust qualitative reproducibility in the composition of the collected media (Supplementary Figure S3A).

Looking for relevant functions and processes that may be related to proteins secreted by SD-MSC, we selected only the proteins identified in at least three samples before following to GO analyses. After that, the most relevant GO terms ($p < 0.001$) from all the analyses were summarized and graphically visualized using the REVIGO tool. The most significant cellular component GO terms were related to "extracellular region part," "vesicles," "extracellular space," and "extracellular matrix" (Figure 1(a)). In this analysis, it was observed that, of the 399 proteins inquired, 366 were related to the "extracellular region" and 94 were associated to "extracellular matrix" (Supplementary Table 2). This shows an enrichment for extracellular proteins in our samples, which is consistent with the fact that we have collected secreted proteins from CMs.

In addition, g:Profiler analysis also identified more than a thousand biological processes. Some of them related to "extracellular matrix organization," "cell proliferation," "immune system," "wound healing," and "blood vessel development" are highlighted in Figure 1(b). Regarding the last two processes, which are directly related to the healing

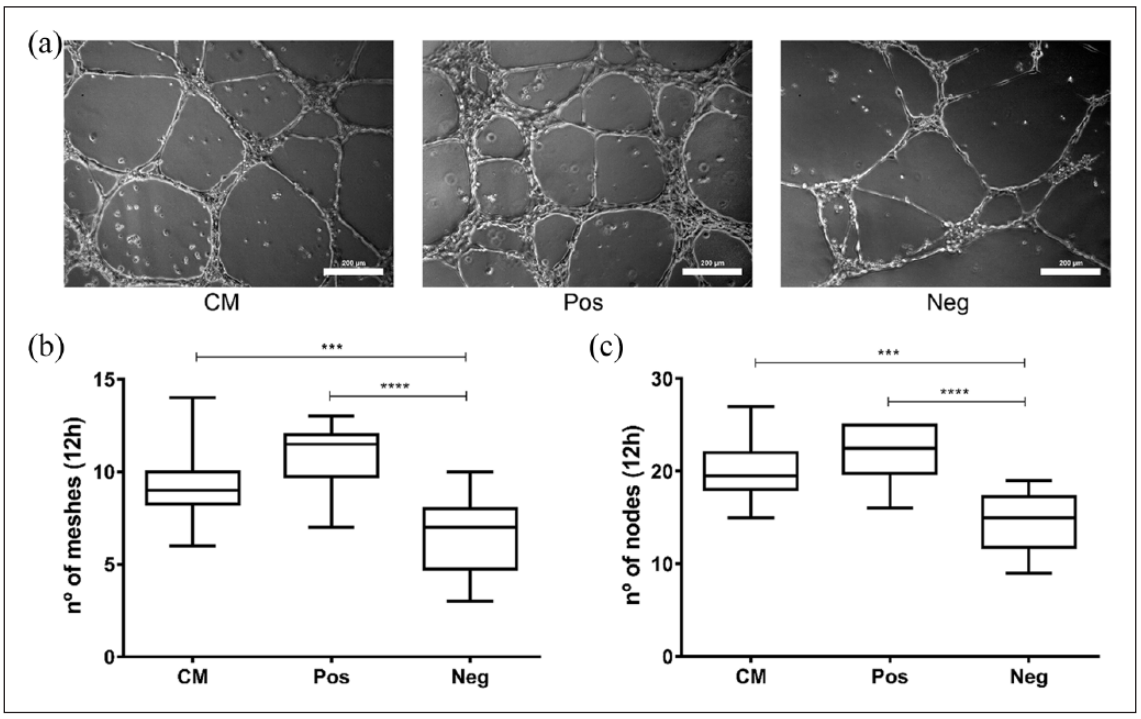

Figure 2. CM derived from SD-MSCs induces tube formation in HUVEC cultures. (a) Representative images of the tubule-like structures that appeared in each condition (200 µm scale bar). Analysis of the number of (b) meshes and (c) nodes formed after 12 h for the CM treatment (CM), positive controls (Pos; EBM-2 fully supplemented, as described in M&M) or negative controls (Neg; EBM-2 without any supplementation). ***$p < 0.001$; ****$p < 0.0001$.

activity, our analysis identified 46 and 48 hits, respectively, in the protein content of SD-MSC-CM. Concerning these proteins, 21 hits are related to both wound healing and angiogenesis, suggesting that they are interconnected processes. Moreover, a more specific analysis within "wound healing" cluster shows that identified proteins are involved in blood coagulation, hemostasis, and platelet aggregation, among other important processes for vascular physiology (Supplementary Table 2). Furthermore, the analysis of molecular functions demonstrated that these proteins are mostly related to "binding" of different types of proteins (such as glycoproteins, collagens, cytokines, and others; Supplementary Table 2 and Supplementary Figure S3B).

SD-MSC-CM stimulates angiogenesis in vitro

The GO terms highlighted in the secretome of SD-MSCs indicated a potential pro-angiogenic effect. We therefore performed an *in vitro* assay with endothelial cells to examine the ability of these cells to generate tubule-like structures. As shown in Figure 2(a), the SD-MSC-CM stimulated the formation of capillary-like tubes in HUVEC cultures. After 12 h, the network of tubule-like structures in CM-treated cultures displayed a similar number of meshes and nodes compared to the positive control (Figure 2(b) and (c)). Although the negative control (non-inductive medium) formed some tubular structures spontaneously, CM and positive control (vascular endothelial growth factor (VEGF)–supplemented inductive medium) cultures exhibited significantly higher and more organized tubule-like structures (Figure 2(a)–(c)). After 24 h, tubule-like structures were almost absent in negative control, but in positive control and CM treatments, they were still remaining (data not shown).

The SD-MSC secretome is sufficient to promote the formation of new blood vessels in vivo

Since SD-MSC-CM induced angiogenesis *in vitro* and highlighted GO terms were also related to wound healing, we verified whether this pro-angiogenic activity and wound repair potential could be observed *in vivo*. Thus, CM was applied to the full thickness of excisional lesions in mice skin. The CM was directly applied to the wounds or embedded within hydrogels to maintain the soluble proteins for longer periods at the wound site. PVA and CG hydrogels were used as CM carriers and were also applied to skin lesions without CM as comparative controls.

On the third day post-treatment, a significant reduction in wound size was observed in animals treated with hydrogels alone compared with untreated animals (Figure 3(a)). Interestingly, animals treated with CG-embedded CM healed slower than mice treated with PVA or CG alone (Figure 3(a)). However, on the 14th day post-treatment, all groups

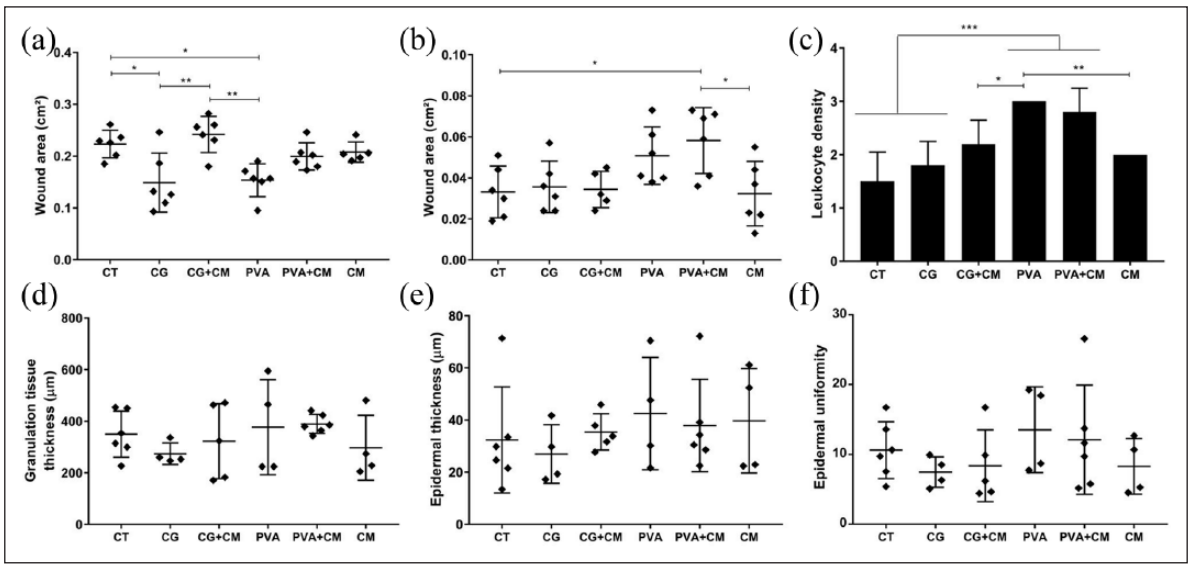

Figure 3. Histomorphological analysis of reepidermalization during skin healing in mice: untreated control (CT) and effects of PVA, carrageenan (CG), conditioned medium (CM), or associations between hydrogels and CM. Wound closure was evaluated by measuring the wound area on the (a) 3rd and (b) 14th day post-treatment. Inflammatory infiltrates were estimated by evaluating the leukocyte density in the lesions on the (c) 3rd day post-treatment (n = 5 animals for each condition). The (d) thickness of granulation tissue and the (e) thickness and (f) uniformity of the epidermis were assessed on the 14th day post-treatment. *$p < 0.05$; **$p < 0.01$; ***$p < 0.001$.

showed successfully repaired and closed wounds, although the animals treated with CM embedded in PVA (or only with PVA) displayed slightly larger wounded areas (Figure 3(b)).

Regarding the inflammatory response, which was evaluated by leukocyte density at the site of the lesion at 3 days post-treatment, the skin of PVA-treated animals (alone or associated with CM) exhibited a higher inflammatory process with denser leukocyte infiltrates than the animals in all other groups (Figure 3(c)). Compared to mice in the untreated control group (CT), mice treated with CM (embedded or not in CG) showed a moderate level of leukocyte density. CG per se did not elicit higher inflammatory responses than that observed in the controls. Furthermore, the thickness of granulation tissue and the thickness and uniformity of the epidermis were not affected by the different treatments on the 14th day post-treatment (Figure 3(d)–(f)).

Although all the experimental groups exhibited similar repaired skin features on the 14th day post-treatment, the number of blood vessels in the granulation tissue was markedly different among the groups. Mice skin treated with CM alone displayed more blood vessels than mice skin treated with hydrogels or untreated animals (Figure 4). In addition, the association of CG hydrogels with the CM (CG + CM) increased the number of blood vessels in the wounds compared to that in the control group. These results confirmed the *in vitro* data and demonstrated that SD-MSC-CM promotes angiogenesis during skin wound healing. Moreover, the association of CM with hydrogels does not improve the effect of CM on wounded skin since no differences were observed regarding the formation of new blood vessels.

Discussion

Stem cell therapy has been widely tested for use to treat a variety of diseases, including skin wound healing.[4,5,31] Notably, the mechanisms underlying tissue regeneration are primarily related to the release of paracrine factors by MSCs.[32] Thus, characterizing the composition of the MSC secretome and investigating the responses it mediates *in vitro* and *in vivo* may help elucidate the mechanisms of tissue regeneration and could promote the development of cell-free therapy. In the present study, we performed a broad characterization of SD-MSC-CM by mass spectrometry and investigated its influence on skin wound healing.

The CM derived from MSCs from different sources has been broadly characterized,[33] but the composition of the SD-MSC secretome requires further investigation. Notably, a recent study employing quantitative proteomics to compare the CM from fetal and adult skin fibroblasts (previously characterized as MSCs) revealed secretome signatures on fetal skin relevant for therapeutic use.[34] In the present study, using LC-MS/MS, we identified more than 300 proteins in each SD-MSC-CM sample. Although most of the proteins have also been previously described in other stem cell secretome analyses, we detected unique protein combinations. Differences

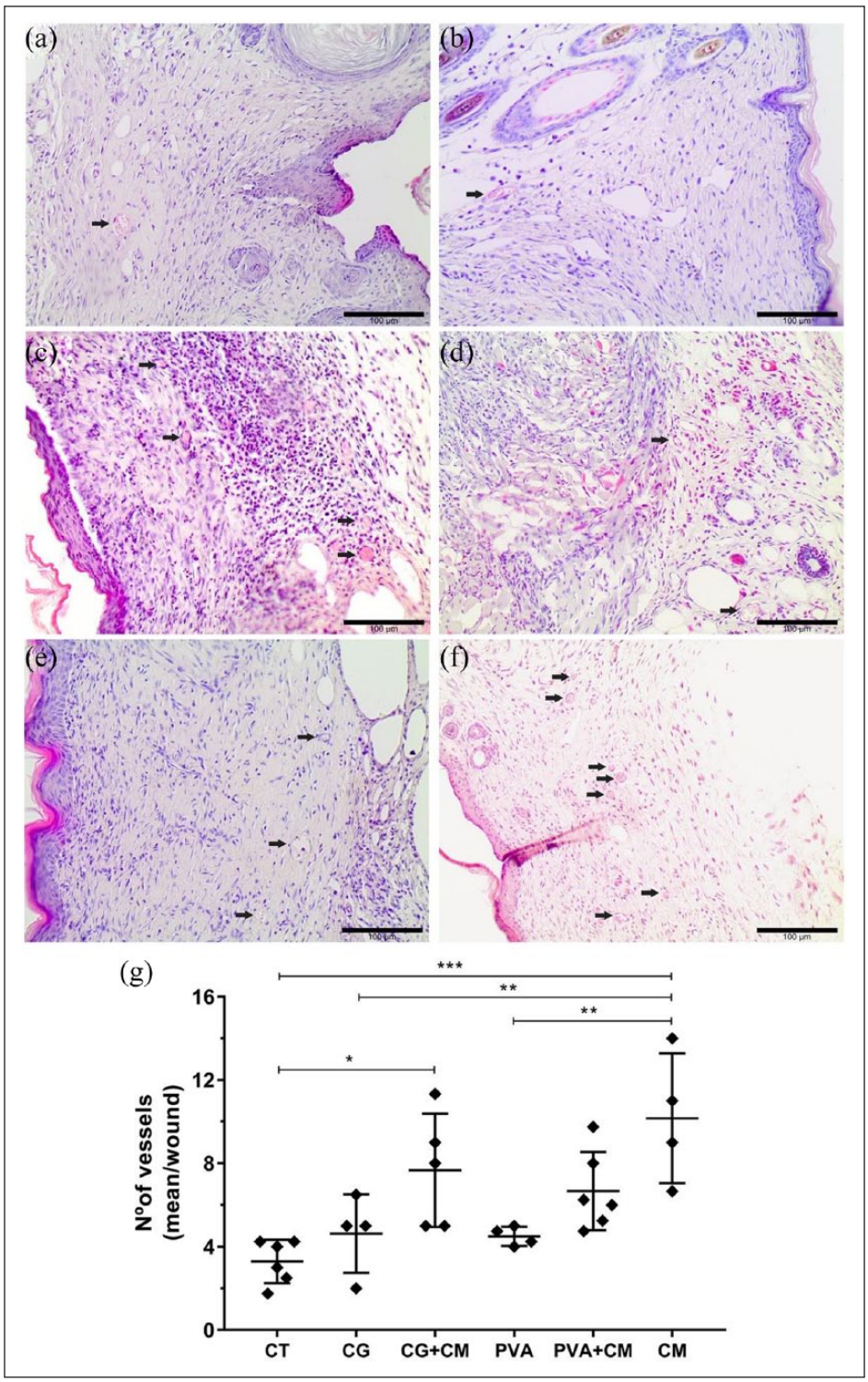

Figure 4. *In vivo* pro-angiogenic effect of the CM derived from SD-MSCs. Representative H&E-stained images of the granulation tissue showing blood vessels (black arrows—capillaries containing a lumen with red blood cells) in the (a) untreated control group (CT) and treated groups: (b) CG, (c) CG + CM, (d) PVA, (e) PVA + CM, and (f) CM. Scale bars = 100 µm. (g) Graph representing the mean values obtained by counting the blood vessels/wound. *$p < 0.05$; **$p < 0.01$; ***$p < 0.001$.

in the CM composition can occur depending on protein identification strategy (antibody arrays, enzyme-linked immunosorbent assay (ELISA), mass spectrometry), CM preparation, protein quality,[35,36] tissue of origin,[37] and cell donor.[38] Such findings strengthen the importance of the characterization of the MSC secretome from different

sources to determine the relevant therapeutic uses of MSC secretomes.

Here, we showed that independent of the cell donor, most of the secreted proteins are similar. The analysis of these proteins highlighted their relation to important processes linked to wound healing, immune system regulation, and blood vessel development. This profile is similar to that of fetal skin cells reported by Gaetani and colleagues that found proteins regulating angiogenesis and wound healing. Their results indicate that these proteins were significantly increased in the secretome of fetal skin cells compared to adult skin cells, suggesting a key possible role of fetal skin cell secretomes toward scarless wound healing.[34] Nevertheless, our data demonstrate that some of the same proteins and other proteins with related functions are constitutively secreted by adult SD-MSCs, indicating that SD-MSC secretomes could be reliable sources of signaling factors modulating wound healing and angiogenesis.

Previously, we have tested SD-MSC and CG, alone or in combination, in the treatment of skin lesion in a murine model of wound healing and showed that the treatment with SD-MSCs induces increasing number of vessels, a fact that was associated with the secretion of soluble factors by MSCs.[20] In this work, we have shown that this pro-angiogenic effect is related to the proteins secreted by SD-MSCs. Angiogenic factors released by MSCs include, among others, the VEGF, angiopoetin-1 (Ang1), insulin-like growth factor 1 (IGF1), fibroblast growth factor 2 (FGF2), hepatocyte growth factor (HGF), transforming growth factor β (TGFβ), monocyte chemoattractant protein 1 (MCP1), interleukin 6 (IL6), endostatin, and stromal cell-derived factor 1 (SDF1, also known as CXCL12).[39–42] In the secretome of SD-MSC, we also identified some of these proteins, such as IL6, HGF, TGFβ, and CXCL12; nevertheless, they did not attend our analysis criteria (they were not present in at least three of the samples or presented only one unique peptide; Supplementary Table 1). Besides that, our methodology for characterization of secreted proteins (label-free mass spectrometry) was different from many of the previous works which verify specifically some proteins using polymerase chain reaction (PCR), ELISA, Luminex, or antibody array. Therefore, this approach has allowed us to find some other proteins directly or indirectly related to wound healing and angiogenesis.

Although the presence of VEGF in the CM derived from MSC cultures indicates its angiogenic potential, the literature has already shown angiogenesis promotion by VEGF-independent responses, as influenced by matrix metalloproteinase 2 (MMP2) found in the CM from umbilical cord-derived MSCs.[40] Also, it has been shown that the angiogenic effect of CM from bone marrow–derived MSC was induced by a set of proteins (e.g. MCP1, IL6, and VEGF) and not by a single inductor.[42] In SD-MSC-CM, we did not identify VEGF, but several proteins with angiogenic potential were found with high expression in the samples (based on Label free Quantification (LFQ) intensities; Supplementary Table 1), among them MMP2 itself. Looking for proteins related to both angiogenesis and wound healing in our data, we found fibronectin (FN1), decorin (DCN), platelet-derived growth factor receptor β (PDGFR β), different types of collagens, and others (Supplementary Table 2). Therefore, the *in vitro* and *in vivo* angiogenic effect fostered by SD-MSC-CM was possibly due to a set of proteins that interact and stimulate cells and other factors at wound lesion site.

The CM derived from MSCs has also been shown to modulate wound healing by inducing the *in vitro* proliferation and migration of monocytes, endothelial cells, and keratinocytes, with corresponding acceleration of wound contraction *in vivo*.[10] Although we have seen some leukocytes increasing at the wounds and the presence of proteins related to wound healing in our results, we did not observe improvements in wound closure, and thickness or uniformity of the epidermis after 14 days of treatment with CM, hydrogels, or their combination. These differences could be related to the delivery method (subcutaneous injection or topical application), methodology for wound injury, the basal medium used to collect CM, and the concentration of proteins in CM, among other factors. In our hands, the most expressive influence of the CM we found was the induction of angiogenesis, both *in vitro* and *in vivo*. In this regard, Yew and colleagues[43] identified p38 Mitogen Activated Protein Kinase (MAPK) as a key signaling pathway in secreting a repertoire of factors, including IL6, IL8, and CXCL1, whose presence was shown to stimulate an increasing capillary density in wound areas. A recent work also demonstrates, in a model of radiation-induced skin wounds in rats, that several repeated applications of CM from Wharton's jelly-derived MSCs could ameliorate wound closure and angiogenesis.[44]

In our previous work, we showed that the association of SD-MSCs with CG allows the permanence of cells at wound site and the possible secretion of healing factors, suggesting CG as a possible delivery vehicle for cells/derivatives.[20] Here, we probed the direct association of the CG hydrogels with SD-MSC-CM, using also PVA hydrogels as a comparative. Nevertheless, our strategy to deliver the secretome embedded in hydrogels did not promote improvements compared to the secretome alone. This approach was recently shown to improve the repair of injured cardiac tissue with an increase in tissue capillary density,[45] although a comparison with the injection of the secretome alone was not performed. Further investigations in this field are required to evaluate the potential interactions and/or activity benefits on secretome–hydrogel associations.

Conclusion

Here, we characterize the secretome from SD-MSCs and demonstrate its protein repertoire associated with possible tissue repair mechanisms (e.g. wound healing, angiogenesis, immune defense response). Mainly, the SD-MSC-CM are

shown to support angiogenic activity *in vitro* and in a preclinical mouse model of cutaneous wound healing, suggesting its potential use in a cell-free therapy. We also showed that the use of CG or PVA hydrogels as well as the delivery of the SD-MSC secretome embedded into them did not improve wound healing or induce better results of tissue vascularization in our *in vivo* model. Then we showed that, at least to our wound healing model, the SD-MSC-CM can be delivered without association with carriers and may act in initial healing response stimulating tissue cells at the wound site.

Author's note

Michele Patricia Rode is now affiliated with Department of Pharmaceutical Sciences, Federal University of Santa Catarina, Florianópolis - SC, Brazil.
Maria Beatriz da Rocha Veleirinho is now affiliated with Plant Morphogenesis and Biochemistry Laboratory, Federal University of Santa Catarina, Florianopolis - SC, Brazil.
Marcelo Maraschinis is now affiliated with Plant Morphogenesis and Biochemistry Laboratory, Federal University of Santa Catarina, Florianopolis - SC, Brazil.
Leila Hayashi is now affiliated with Department of Aquaculture, Federal University of Santa Catarina, Florianópolis - SC, Brazil.

Acknowledgements

We would like to thank all the staff of the Carlos Chagas Institute, Oswaldo Cruz Foundation at Paraná (FIOCRUZ-PR) and the Federal University of Santa Catarina (UFSC) for the laboratory and administrative support. We thank the Program for Technological Development in Tools for Health-PDTIS-FIOCRUZ for use of its facilities.

Declaration of conflicting interests

The author(s) declared no potential conflicts of interest with respect to the research, authorship, and/or publication of this article.

Funding

The author(s) disclosed receipt of the following financial support for the research, authorship, and/or publication of this article: This work was funded by the National Council of Technological and Scientific Development (CNPq process 445890/2014-2) and the Foundation for Research and Innovation Support of the State of Santa Catarina (FAPESC/TO 2015TR309).

Supplemental material

Supplemental material for this article is available online.

ORCID iDs

Giordano Wosgrau Calloni https://orcid.org/0000-0003-3954-0808
Marco Augusto Stimamiglio https://orcid.org/0000-0001-8537-2812

References

1. Da LC, Huang YZ and Xie HQ. Progress in development of bioderived materials for dermal wound healing. *Regen Biomater* 2017; 4(5): 325–334.
2. MacNeil S. Progress and opportunities for tissue-engineered skin. *Nature* 2007; 445(7130): 874–880.
3. Jayaraman P, Nathan P, Vasanthan P, et al. Stem cells conditioned medium: a new approach to skin wound healing management. *Cell Biol Int* 2013; 37(10): 1122–1128.
4. Abo-Elkheir W, Hamza F, Elmofty AM, et al. Role of cord blood and bone marrow mesenchymal stem cells in recent deep burn: a case-control prospective study. *Am J Stem Cells* 2017; 6(3): 23–35.
5. François S, Eder V, Belmokhtar K, et al. Synergistic effect of human bone morphogenic protein-2 and mesenchymal stromal cells on chronic wounds through hypoxia-inducible factor-1 α induction. *Sci Rep* 2017; 7: 4272.
6. Mehanna RA, Nabil I, Attia N, et al. The effect of bone marrow-derived mesenchymal stem cells and their conditioned media topically delivered in fibrin glue on chronic wound healing in rats. *Biomed Res Int* 2015; 2015: 846062.
7. Dong L, Hao H, Liu J, et al. A conditioned medium of umbilical cord mesenchymal stem cells overexpressing Wnt7a promotes wound repair and regeneration of hair follicles in mice. *Stem Cells Int* 2017; 2017: 3738071.
8. Kim J, Lee JH, Yeo SM, et al. Stem cell recruitment factors secreted from cord blood-derived stem cells that are not secreted from mature endothelial cells enhance wound healing. *In Vitro Cell Dev Biol Anim* 2014; 50: 146–154.
9. Walter MNM, Wright KT, Fuller HR, et al. Mesenchymal stem cell-conditioned medium accelerates skin wound healing: an in vitro study of fibroblast and keratinocyte scratch assays. *Exp Cell Res* 2010; 316(7): 1271–1281.
10. Chen L, Tredget EE, Wu PYG, et al. Paracrine factors of mesenchymal stem cells recruit macrophages and endothelial lineage cells and enhance wound healing. *PLoS ONE* 2008; 3(4): e1886.
11. Park SR, Kim JW, Jun HS, et al. Stem cell secretome and its effect on cellular mechanisms relevant to wound healing. *Mol Ther* 2018; 26(2): 606–617.
12. Lee K, Silva EA and Mooney DJ. Growth factor delivery-based tissue engineering: general approaches and a review of recent developments. *J R Soc Interface* 2011; 8(55): 153–170.
13. Koria P. Delivery of growth factors for tissue regeneration and wound healing. *Biodrugs* 2012; 26(3): 163–175.
14. Nguyen MK and Alsberg E. Bioactive factor delivery strategies from engineered polymer hydrogels for therapeutic medicine. *Prog Polym Sci* 2014; 39(7): 1236–1265.
15. Campo VL, Kawano DF, Silva DB, et al. Carrageenans: biological properties, chemical modifications and structural analysis—a review. *Carbohydr Polym* 2009; 77: 167–180.
16. Grenha A, Gomes ME, Rodrigues M, et al. Development of new chitosan/carrageenan nanoparticles for drug delivery applications. *J Biomed Mater Res A* 2010; 92(4): 1265–1272.
17. Santo VE, Frias AM, Carida M, et al. Carrageenan-based hydrogels for the controlled delivery of PDGF-BB in bone tissue engineering applications. *Biomacromolecules* 2009; 10(6): 1392–1401.
18. Popa EG, Gomes ME and Reis RL. Cell delivery systems using alginate–carrageenan hydrogel beads and fibers for regenerative medicine applications. *Biomacromolecules* 2011; 12: 3952–3961.

19. Yegappan R, Selvaprithiviraj V, Amirthalingam S, et al. Carrageenan based hydrogels for drug delivery, tissue engineering and wound healing. *Carbohydr Polym* 2018; 198: 385–400.
20. Rode MP, Batti Angulski AB, Gomes FA, et al. Carrageenan hydrogel as a scaffold for skin-derived multipotent stromal cells delivery. *J Biomater Appl* 2018; 33(3): 422–434.
21. Alves M-H, Jensen BEB, Smith AAA, et al. Poly(vinyl alcohol) physical hydrogels: new vista on a long serving biomaterial. *Macromol Biosci* 2011; 11(10): 1293–1313.
22. Kamoun EA and Kenawy Chen X. A review on polymeric hydrogel membranes for wound dressing applications: PVA-based hydrogel dressings. *J Adv Res* 2017; 8(3): 217–233.
23. Kamoun EA, Chen X, Mohy MS, et al. Crosslinked poly(vinyl alcohol) hydrogels for wound dressing applications: a review of remarkably blended polymers. *Arab J Chem* 2015; 8: 1–14.
24. Nkhwa S, Lauriaga KF, Kemal E, et al. Poly(vinyl alcohol): physical approaches to designing biomaterials for biomedical applications. *Conf Pap Sci* 2014; 2014: 403472.
25. Cutiongco MFA, Choo RKT, Shen NJX, et al. Composite scaffold of poly(vinyl alcohol) and interfacial polyelectrolyte complexation fibers for controlled biomolecule delivery. *Front Bioeng Biotechnol* 2015; 3: 3.
26. Jeremias Tda S, Machado RG, Visoni SB, et al. Dermal substitutes support the growth of human skin-derived mesenchymal stromal cells: potential tool for skin regeneration. *PLoS ONE* 2014; 9(2): e89542.
27. Reus TL, Robert AW, DaCosta MB, et al. Secretome from resident cardiac stromal cells stimulates proliferation, cardiomyogenesis and angiogenesis of progenitor cells. *Int J Cardiol* 2016; 221: 396–403.
28. Reimand J, Arak T, Adler P, et al. g:Profiler—a web server for functional interpretation of gene lists (2016 update). *Nucleic Acids Res* 2016; 44: W83–W8.
29. Supek F, Bošnjak M, Škunca N, et al. Revigo summarizes and visualizes long lists of gene ontology terms. *PLoS One*; 6. Epub ahead of print 2011. DOI: 10.1371/journal.pone.0021800.
30. Wang X, Ge J, Tredget EE, et al. The mouse excisional wound splinting model, including applications for stem cell transplantation. *Nat Protoc* 2013; 8(2): 302–309.
31. Zahorec P, Koller J, Danisovic L, et al. Mesenchymal stem cells for chronic wounds therapy. *Cell Tissue Bank* 2015; 16: 19–26.
32. Gnecchi M, Danieli P, Malpasso G, et al. *Paracrine mechanisms of mesenchymal stem cells in tissue repair*. New York: Humana Press, pp. 123–146.
33. Skalnikova H, Motlik J, Gadher SJ, et al. Mapping of the secretome of primary isolates of mammalian cells, stem cells and derived cell lines. *Proteomics* 2011; 11(4): 691–708.
34. Gaetani M, Chinnici CM, Carreca AP, et al. Unbiased and quantitative proteomics reveals highly increased angiogenesis induction by the secretome of mesenchymal stromal cells isolated from fetal rather than adult skin. *J Tissue Eng Regen Med* 2018; 12(2): e949–e961.
35. Lavoie JR and Rosu-Myles M. Uncovering the secrets of mesenchymal stem cells. *Biochimie* 2013; 95(12): 2212–2221.
36. Kupcova Skalnikova H. Proteomic techniques for characterisation of mesenchymal stem cell secretome. *Biochimie* 2013; 95(12): 2196–2211.
37. Pires AO, Mendes-Pinheiro B, Teixeira FG, et al. Unveiling the differences of secretome of human bone marrow mesenchymal stem cells, adipose tissue-derived stem cells, and human umbilical cord perivascular cells: a proteomic analysis. *Stem Cells Dev* 2016; 25(14): 1073–1083.
38. Assoni A, Coatti G, Valadares MC, et al. Different donors mesenchymal stromal cells secretomes reveal heterogeneous profile of relevance for therapeutic use. *Stem Cells Dev* 2017; 26(3): 206–214.
39. Hsiao ST, Asgari A, Lokmic Z, et al. Comparative analysis of paracrine factor expression in human adult mesenchymal stem cells derived from bone marrow, adipose, and dermal tissue. *Stem Cells Dev* 2012; 21(12): 2189–2203.
40. Kuchroo P, Dave V, Vijayan A, et al. Paracrine factors secreted by umbilical cord-derived mesenchymal stem cells induce angiogenesis in vitro by a VEGF-independent pathway. *Stem Cells Dev* 2015; 24(4): 437–450.
41. Amable P, Teixeira MV, Carias RB, et al. Protein synthesis and secretion in human mesenchymal cells derived from bone marrow, adipose tissue and Wharton's jelly. *Stem Cell Res Ther* 2014; 5(2): 53.
42. Kwon HM, Hur S, Park K, et al. Multiple paracrine factors secreted by mesenchymal stem cells contribute to angiogenesis. *Vasc Pharmacol* 2014; 63(1): 19–28.
43. Yew TL, Hung YT, Li HY, et al. Enhancement of wound healing by human multipotent stromal cell conditioned medium: the paracrine factors and p38 MAPK activation. *Cell Transp* 2011; 20(5): 693–706.
44. Sun J, Zhang Y, Song X, et al. The healing effects of conditioned medium derived from mesenchymal stem cells on radiation-induced skin wounds in rats. *Cell Transp*. Epub ahead of print 23 October 2018. DOI: 10.1177/0963689718807410.
45. Waters R, Alam P, Pacelli S, et al. Stem cell-inspired secretome-rich injectable hydrogel to repair injured cardiac tissue. *Acta Biomater* 2018; 69: 95–106.